Search for the critical point of strongly interacting matter

(Proton and pion intermittency analysis by NA61/SHINE at CERN SPS)

A Haradhan

Jan Kochanowski University, Kielce

May 17, 2023

Phase diagrams

Strongly interacting matter: system of strongly interacting particles in equilibrium governed by the strong interaction (fundamental forces in nature and is responsible for the binding of protons and neutrons into nuclei and quarks and gluons into hadrons)

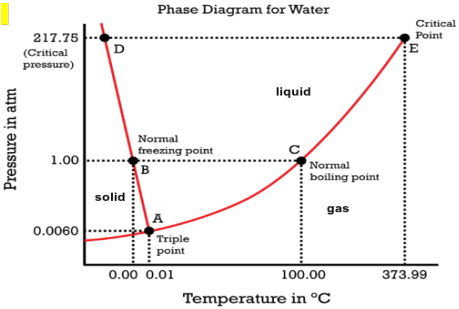

- **Water phase diagram:** different phases of water at equilibrium governed by electromagnetic interaction
- **Phases:** solid, liquid, and gas
- **Water CP:** a line of first-order liquid-gas transitions ends, and the transition becomes second-order, and the difference between the liquid and gas phases disappears

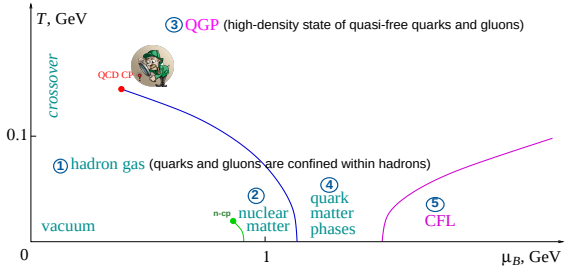

- **QCD Phase diagram:** system of strongly interacting particles in equilibrium governed by the strong interaction
- **Phases:** HG, nuclear matter, QGP ,quark-matter, CFL phase
- **QCD CP:** hypothetical end-point of the first-order phase line between HG and QGP that has properties of a second-order phase transition and then turns into a crossover

Phase diagrams

Strongly interacting matter: system of strongly interacting particles in equilibrium governed by the strong interaction (fundamental forces in nature and is responsible for the binding of protons and neutrons into nuclei and quarks and gluons into hadrons)

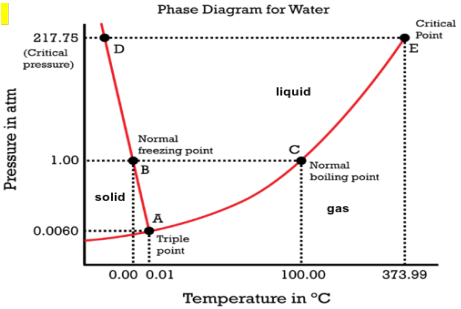

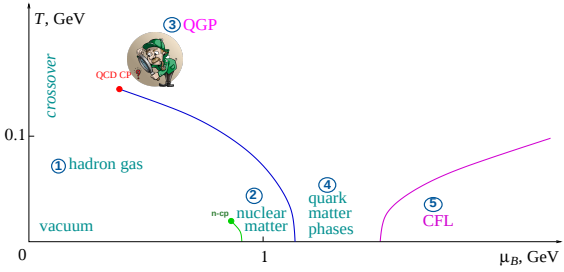

- **Water phase diagram:** different phases of water at equilibrium governed by electromagnetic interaction
- **Phases:** solid, liquid, and gas
- **Water CP:** a line of first-order liquid-gas transitions ends, and the transition becomes second-order, and the difference between the liquid and gas phases disappears

- **QCD Phase diagram:** system of strongly interacting particles in equilibrium governed by the strong interaction
- **Phases:** HG, nuclear matter, QGP ,quark-matter, CFL phase
- **QCD CP:** hypothetical end-point of the first-order phase line between HG and QGP that has properties of a second-order phase transition and then turns into a crossover

Location of QCD CP from models and lattice QCD calculations

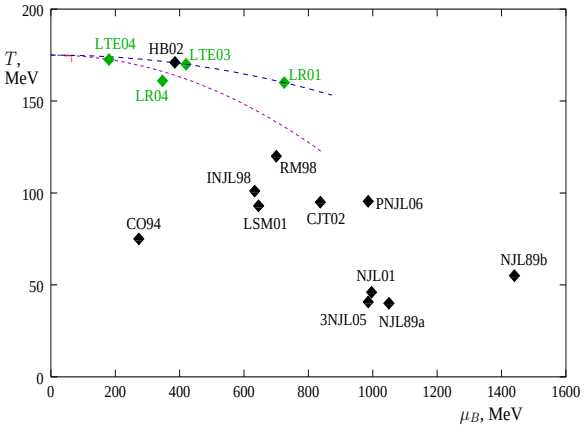

Summary of many model calculations to predict the location of QCD CP on the phase diagram

- Different models approaches indicate that the transition in this region is strongly first-order and has properties of a second-order phase transition

  Asakawa and Yazaki: Nucl. Phys. A 504 (1989)
  A. Barducci et al.: Phys. Rev. D 41 (1990), p. 1610

- First order line originating at zero T cannot end at the vertical axis $\mu_B = 0$, the line must end in the middle of the diagram
- Most of the theoretical knowledge of the phase diagram is restricted to the vicinity of $\mu_{\mathbf{B}} = 0$ (lattice QCD methods)
- Lattice QCD at a finite μ_B is exponentially difficult due to the well-known sign problem,
- Lattice QCD approaches:
  1) simulations at finite imaginary values of μ_B
  2) Taylor expansions around $\mu_B = 0$
- First lattice QCD prediction:
  $T^{CP} = 160 \pm 3.5$ MeV and $\mu_B^{CP} = 725 \pm 35$ MeV

  Fodor and Katz: JHEP 03 (2002), p. 014
- Latest lattice QCD prediction: $T^{CP} < 130$ MeV, $\mu_B^{CP} > 400$ MeV
- Calculations from both lattice QCD approaches in-agreement for $\mu_B/T \leq 2$ - 2.5

  Frithjof Karsch: arXiv: 2212.03015

Location of QCD CP from models and lattice QCD calculations

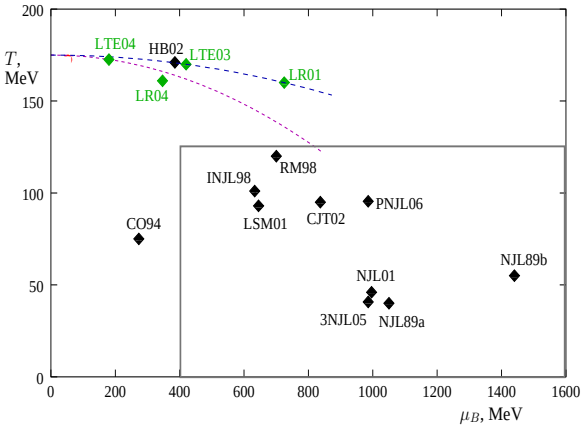

Summary of many model calculations to predict the location of QCD CP on the phase diagram

- Different models approaches indicate that the transition in this region is strongly first-order and has properties of a second-order phase transition

  Asakawa and Yazaki: Nucl. Phys. A 504 (1989)
  A. Barducci et al.: Phys. Rev. D 41 (1990), p. 1610

- First order line originating at zero T cannot end at the vertical axis $\mu_B = 0$, the line must end in the middle of the diagram
- Most of the theoretical knowledge of the phase diagram is restricted to the vicinity of $\mu_{\mathbf{B}} = 0$ (lattice QCD methods)
- Lattice QCD at a finite μ_B is exponentially difficult due to the well-known sign problem,
- Lattice QCD approaches:
  1) simulations at finite imaginary values of μ_B
  2) Taylor expansions around $\mu_B = 0$
- First lattice QCD prediction:
  $T^{CP} = 160 \pm 3.5$ MeV and $\mu_B^{CP} = 725 \pm 35$ MeV

  Fodor and Katz: JHEP 03 (2002), p. 014
- Latest lattice QCD prediction: $T^{CP} < 130$ MeV, $\mu_B^{CP} > 400$ MeV
- Calculations from both lattice QCD approaches in-agreement for $\mu_B/T \leq 2$ - 2.5

  Frithjof Karsch: arXiv: 2212.03015

Experimental search for the QCD critical point

1. Does the QCD CP exist in nature?
2. Where is it located in the QCD phase diagram?

Experimental QCD CP search

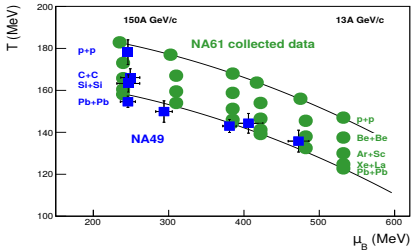

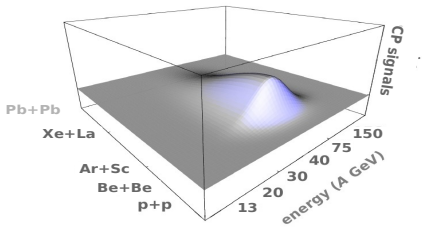

- At the QCD CP, correlation length, $\xi \to \infty$ and the system becomes scale-invariant $\Longrightarrow$ substantial fluctuations in particle multiplicity
- QCD CP signatures can be observed if the freeze-out point (at the stage where the final hadrons are emitted) is located close to QCD CP
- Location of the freeze-out point depends on the collision energy and size of the colliding nuclei
- Experimental search for the QCD CP requires a two-dimensional scan of collision energy and size of the colliding nuclei
- While scanning a phase diagram, maximum of the characteristic fluctuation signals of the QCD CP is located at the hill

NA61/SHINE's QCD CP search tools

1. **Multiplicity fluctuations in a large momentum acceptance:**

   - **Intensive quantities:** system size and energy dependence of second, third and fourth order cumulant ratio of net-electric charge in $p+p$, central Be+Be and Ar+Sc interactions by NA61/SHINE
     - - no signature of QCD CP
   - **Strongly-intensive quantities:** system size dependence of strongly intensive quantities from the NA49 and NA61/SHINE experiment as a function of system size
     - - no signature of QCD CP

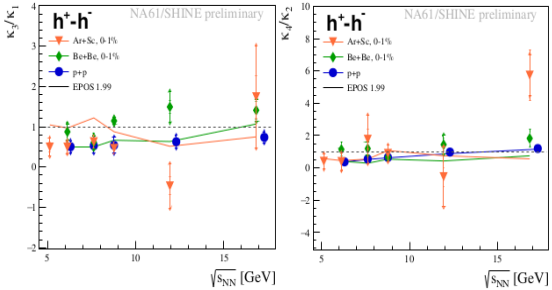

2. **Short-range correlation (HBT analysis) :**

   transverse-mass (m_T) dependence of Levy exponent α has been studied both at SPS and RHIC
   - - no signature of QCD CP

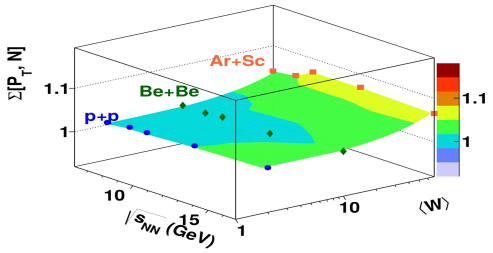

3. **Ongoing intermittency analysis:**

   NA61/SHINE experiment performs a systematic scan in collision energy and system size through the analysis of the scaled factorial moments (SFMs) of the second and higher orders as a function of the phase space cell size in the transverse momentum plane

Intermittency

Intermittency: random deviations from smooth or regular behaviour

H Satz: Nuclear Physics B326 (1989) 613-618

Let's consider putting N balls into a box of size Δ

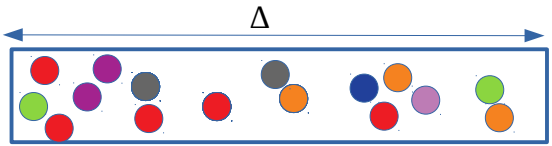

Intermittency

Intermittency: random deviations from smooth or regular behaviour

H Satz: Nuclear Physics B326 (1989) 613-618

Let's consider putting N balls into a box of size Δ

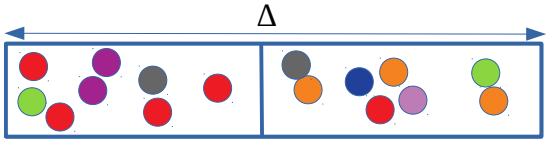

Question: what will happen when varying number of cells (M) but the length of the box Δ and total number of balls (N) are fixed ??

Intermittency

Intermittency: random deviations from smooth or regular behaviour

H Satz: Nuclear Physics B326 (1989) 613-618

Let's consider putting N balls into a box of size Δ

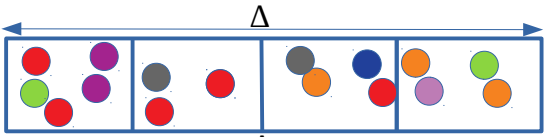

Intermittency

Intermittency: random deviations from smooth or regular behaviour

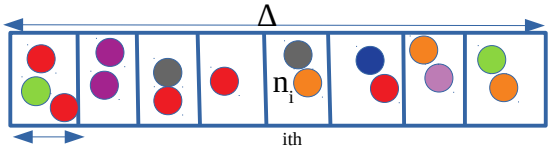

N: total number of balls

Δ: size of the box

δ: size of each cell

M (Δ/δ): number of cells

n_i : number of balls puts into ith cell such that $\sum_i n_i = N$

The r-order moment for a given configuration (a given distribution of the balls) is defined as:

$$f_r(M) = \frac{\left[\frac{1}{M}\sum_{i=1}^{M} n_i^r\right]}{\left[\frac{1}{M}\sum_{i=1}^{M} n_i\right]^r} = M^{r-1}N^{-1}\sum_{i=1}^{M} n_i^r \qquad (1)$$

Intermittency

Case 1: equidistribution (N/M balls in each box)

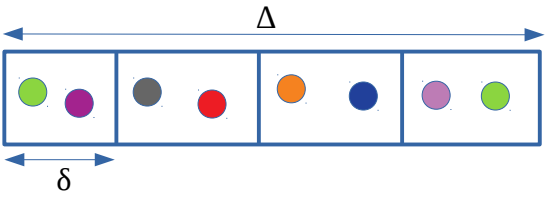

$$n_i = N/M \ , \forall i$$

$$f_r(M) = 1, \ \forall i$$

Case 2: all balls into one cell (for an extreme fluctuation, from a thermodynamic point of view)

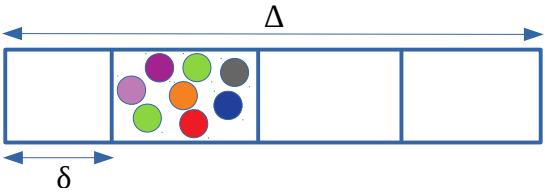

$$n_i = N \text{ for } i = 2$$

$$n_i = 0 \text{ for } i \neq 2$$

$$f_r(M) = M^{r-1}$$

$$log\ (f_r(M)) = -(r-1)\ log(\delta) + (r-1)\ log(\Delta)$$

Intermittent: $log(f_r(M))$ varies linearly with $log(\delta)$

Intermittency indices: coefficient of $log(\delta)$

History of Intermittency analysis in high energy physics

- Concept of intermittency was originally developed in the study of turbulent flow
  Ya.B. Zel'dovich et al., Usp. Fiz. Nauk 152 (1987) 3
- In the pioneering article of Bialas and Peschanski, intermittency analysis was introduced to high-energy physics to study fluctuations
  Bialas and Peschansk: Nucl. Phys. B 273 (1986),1496 pp. 703–718
- It was proposed to study the scaled factorial moments of rapidity distribution of particles produced in high-energy collision as a function of the resolution (size of rapidity interval)
- The pioneering work of Wosiek found indications of intermittent behaviour in the critical region of the two-dimensional Ising model
  Wosiek: Acta Physica Polonica, Series B1670 19.10 (1988), pp. 863–866
- This raised the general question of whether or not intermittency and critical behaviour are related. Satz showed that the critical behaviour of the Ising model indeed leads to intermittency, with indices determined by the critical exponents
- Bialas and Hwa reported that intermittency parameters could serve as a signal of second-order phase transition using scaled factorial moments
  Bialas and Hwa: Phys.Lett. B253 (1991), pp. 436–438

Scaled factorial moments of order r

second-order phase transition, the correlation length diverge $\longrightarrow$ system becomes scale-invariant$\longrightarrow$ enhanced multiplicity fluctuations that can be revealed by scaled factorial moments

$$F_r(M) = \frac{\left\langle \frac{1}{M}\sum_{i=1}^{M} n_i(n_i-1)...(n_i-r+1) \right\rangle}{\left\langle \frac{1}{M}\sum_{i=1}^{M} n_i \right\rangle^r}$$

n_i: numbers of particles in ith bin

$< .... >$: averaging over events

M: number of subdivision intervals of the selected range Δ

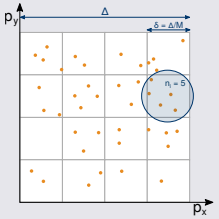

When the system is a simple fractal and $F_r(M)$ follows a power law dependence:

$$F_r(M) = F_r(\Delta) \cdot M^{\varphi_r}$$

where critical exponent or intermittency index, φ_r obeys the relation:

$$\varphi_r = (r-1) \cdot d_r$$

where the anomalous fractal dimension d_r is independent of r

Wosiek, APPB 19 (1988) 863

Bialas, Hwa, PLB 253 (1991) 436

Bialas,Peschanski, NPB 273(1986) 703

Antoniou, Diakonos, Kapoyannis, Kousouris, PRL 97 (2006) 032002

Scaled factorial moments and mixed data sets

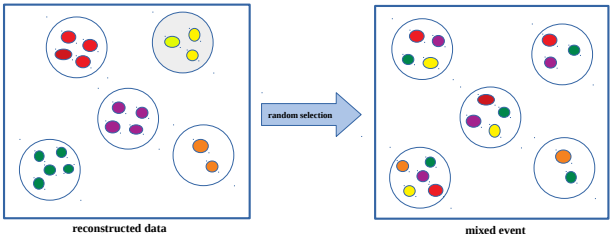

- Mixed data set is constructed by randomly swapping particles from different events so that each particle in each mixed event comes from different recorded events but keeps multiplicity as the recorded data set
- Event mixing is used to remove correlations between particles

- If the system is self-similar, $F_2(M) \sim M^{\varphi_2}$
- Theoretical expectation value for $\varphi_2 = 5/6$

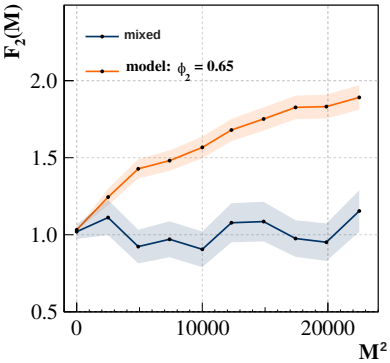

Proton intermittency results from NA49

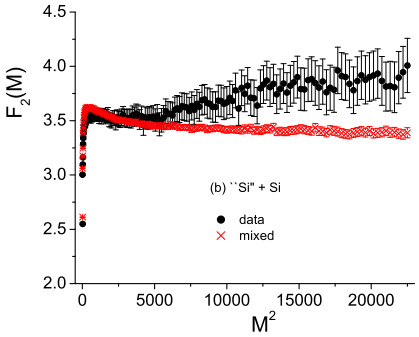

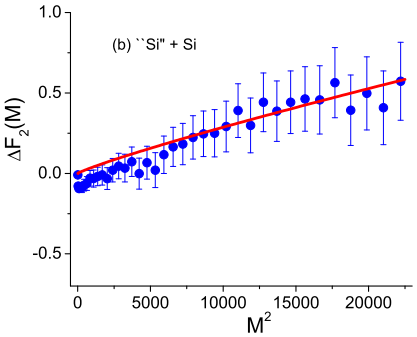

- Non-cumulative transverse momenta are use, to remove all possible dynamical correlations: $\Delta F_2(M) = F_2^{data}(M) - F_2^{data}(M)$
- This resulted in statistically correlated data points uncertainties, therefore the full covariance matrix is required for proper statistical treatment of the results
- Power-law fit in the region $M^2 > 6000$ gave the result $\varphi_2 = 0.96^{+0.38}_{-0.25}(stat) \pm 0.16(syst)$ with $\chi^2/d.o.f \approx 0.09$ - 0.51

NA61/SHINE detector

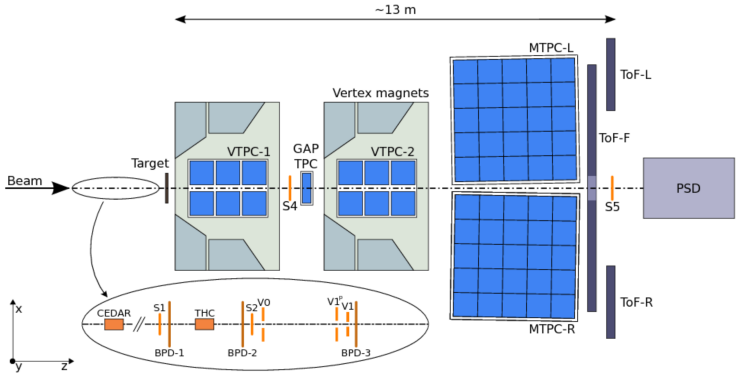

- NA61/SHINE (**S**PS **H**eavy **I**on and **N**eutrino **E**xperiment) is a particle physics fixed-target experiment at CERN SPS
- Time projection chamber (TPC) system: track reconstruction and particle identification based on specific energy loss
- VTPC-1, and VTPC-2 are placed in the magnetic field: used for tracks momentum reconstruction
- Projectile Spectator Detector (PSD): hadronic calorimeter, measures projectile spectator's energy

N. Abgrall et al., [NA61/SHINE Collab.] arXiv:1401.4699 [physics.ins-det]

Analysis of NA61/SHINE's Ar+Sc and Pb+Pb data sets

Ar+Sc collisions collected in 2015 at:

$$\begin{aligned} p_{beam} &= 13A \text{ GeV}/c \ (\sqrt{s_{NN}} \approx 5.12 \text{ GeV}), \\ &= 19A \text{ GeV}/c \ (\sqrt{s_{NN}} \approx 6.12 \text{ GeV}), \\ &= 30A \text{ GeV}/c \ (\sqrt{s_{NN}} \approx 7.62 \text{ GeV}), \\ &= 40A \text{ GeV}/c \ (\sqrt{s_{NN}} \approx 8.77 \text{ GeV}), \\ &= 75A \text{ GeV}/c \ (\sqrt{s_{NN}} \approx 11.9 \text{ GeV}), \end{aligned}$$

Pb+Pb collisions collected in 2016 at:

$$\begin{aligned} p_{beam} &= 13A \text{ GeV}/c \ (\sqrt{s_{NN}} \approx 5.12 \text{ GeV}), \\ &= 30A \text{ GeV}/c \ (\sqrt{s_{NN}} \approx 7.62 \text{ GeV}), \end{aligned}$$

Data production used for this analysis:

- $13A$ GeV/c:032_17c_v1r10p0_pA_slc6_final
- $19A$ GeV/c:028_17c_v1r7p0_pA_slc6_phys
- $30A$ GeV/c:026_17b_v1r7p0_pA_slc6_phys
- $40A$ GeV/c:025_17b_v1r6p0_pA_slc6_phys
- $75A$ GeV/c:026_17b_v1r6p0_pA_slc6_phys

- Data production and location can be found here: https://twiki.cern.ch/twiki/bin/view/NA61/CalibProds2015
- Event selection (to select events contain well-reconstructed central Ar+Sc interactions): https://gitlab.cern.ch/na61-software/framework/Shine/tree/master/Applications/Standard/Analysis/EventCutsArSc
- Event selection of Pb+Pb at $13A$ and $30A$ GeV/c (Centrality: 0-10%): https://indico.cern.ch/event/1277154/contributions/5378937/attachments/2636024/4560373/Event_Selection_PbPb13A&30A.pdf
- Standard track selection (to select tracks of primary charged hadrons and to reduce the contamination by particles from secondary interactions, weak decays and off-time interactions): https://twiki.cern.ch/twiki/bin/view/NA61/Intermittency_PbPb13A

Proton candidates selection

Example: Ar+Sc at 75*A* GeV/*c*

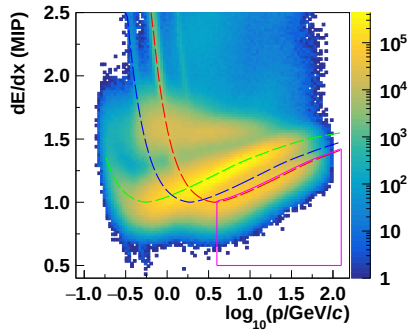

- - - - - : theoretical BB function for protons

- - - - - : theoretical BB function for kaons

- - - - - : theoretical BB function for pions

————: dEdx cut based on BB

selection of protons is based on dEdx measurements in TPCs

- $0.60 < log_{10}(p/GeV/c) < 2.10$ or $(3.98 < p < 125.90)$
- $0.5 \leq$ dEdx $\leq BB_{proton} + 0.15(\ BB_{kaon}$ - $BB_{proton})$

p_{beam} (GeV/c)	*average fraction of protons(%)	average kaon contamination(%)
13A	63	3
19A	63	3
30A	63	3
40A	62	4
75A	62	3
150A	60	4

* average was done over p-p_T acceptance of this analysis

Similar procedure was used to select proton candidates for Ar+Sc at 13*A*-150*A* GeV/*c*

BB: theoretical Bethe-Bloch function

Single particle acceptance map

Three-dimensional (3D) acceptance maps (in center-of-mass rapidity, p_x and p_y) are created to describe momentum region selected for proton intermittency analysis for Pb+Pb at 13A, 30A GeV/c and Ar+Sc at 13A -150A GeV/c data

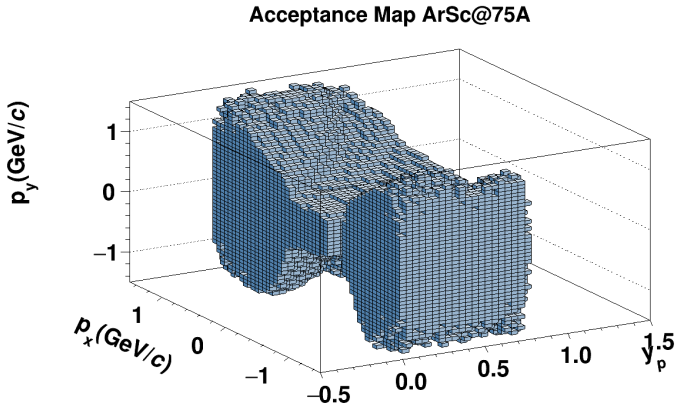

These single-particle acceptance maps should use for model comparison

Two particle acceptance map

- TPCs are not capable of distinguishing tracks that are too close to each other in space and at a small distance, clusters overlap, and signals are merged
- To calculate geometrical two-track distance, requires knowledge of the NA61/SHINE detector geometry and magnetic field
- Momentum of each positive particle in both recorded and mixed data sets in the new momentum co-ordinate $s_x(\frac{p_x}{p_{xz}})$, $s_y(\frac{p_y}{p_{xz}})$, and $\rho(\frac{1}{p_{xz}})$
- particle pairs with momenta inside all the following ellipses with numerical cut values are rejected

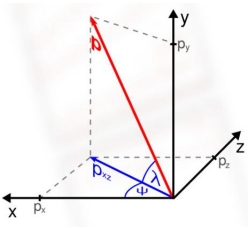

$$\left(\frac{\Delta\rho}{r_\rho}\right)^2 + \left(\frac{\Delta s_y}{r_{s_y}}\right)^2 \leq 1$$

$$\left(\frac{\Delta s_x}{r_{s_x}}\right)^2 + \left(\frac{\Delta s_y}{r_{s_y}}\right)^2 \leq 1$$

$$\left(\frac{\Delta\rho\cos\theta - \Delta s_x \sin\theta}{r_{\rho s_x}}\right)^2 + \left(\frac{\Delta\rho\sin\theta + \Delta s_x\cos\theta}{r_{s_x\rho}}\right)^2 \leq 1$$

p_{beam} (GeV/c)	r_ρ	r_{s_y}	r_{s_x}	$r_{\rho s_x}$	$r_{s_x\rho}$	θ
13A	0.470	0.004	0.047	0.470	0.004	5
19A	0.121	0.003	0.010	0.121	0.003	8
30A	0.123	0.002	0.013	0.123	0.002	13
40A	0.043	0.002	0.010	0.043	0.002	15
75A	0.080	0.002	0.011	0.0200	0.002	31
150A	0.0105	0.0018	0.0080	0.0200	0.0023	51

These two-particle acceptance maps should be used for comparison of experimental results with a model

Proton intermittency analysis methodology

Proton intermittency analysis key points: proton multiplicity fluctuations are studied,

- in transverse momentum plane ($p_x - p_y$ plane)
  Bialas and Seixas: Phys. Lett. B1498 250 (1990), pp. 161–163
- at mid-rapidity
  Antoniou, Diakonos, and Kapoyannis: Phys.Rev. C81 (2010), p. 011901
- using cumulative transformation of transverse momenta
  Bialas and Gazdzicki: Phys. Lett.1490 B 252 (1990), pp. 483–486
- independent sub-sample used for each data point
  H. Adhikary et. al.(NA61/SHINE Collaboration:) arXiv:2305.07557v1
- up-to $r = 2$, $F_2(M)$ due to low proton multiplicity

$$F_2(M) = 2M^2 \frac{\langle N_2(M) \rangle}{\langle N \rangle^2},$$

Statistical error propagation:

$$\frac{\sigma_{F_2}}{|F_2|} = \sqrt{\frac{(\sigma_{N_2})^2}{\langle N_2 \rangle^2} + 4\frac{(\sigma_N)^2}{\langle N \rangle^2} - 4\frac{(\sigma_{N_2 N})^2}{\langle N \rangle \langle N_2 \rangle}}.$$

M: number of bins in p_x and p_y

N: event multiplicity

$< \ldots . >$: averaging over events

N_2: total number of pairs in M bins in an event

Independent sub-sample for each M points

statistically-independent data subsets were used to obtain results for each subdivision number:

- Results for different subdivision numbers are statistically independent
- Complete relevant information needed to interpret the results is easy to present graphically (only diagonal elements of the covariance matrix are non-zero)
- But this procedure significantly decreases the number of events used to calculate each data point increasing statistical uncertainties and therefore forcing to reduce the number of the data points to 10

number of bins	1^2	50^2	70^2	86^2	100^2	111^2	122^2	132^2	141^2	150^2
fraction of all events (%)	0.5	3.0	5.0	7.0	9.0	11.0	13.0	15.5	17.0	19.0

Cumulative variables

Scaled factorial moments are sensitive to the shape of the single-particle momentum distribution and it may bias the signal of critical fluctuation. To remove this dependence:

- construct a mixed events data set and calculate $\Delta F_2(M) = F_2^{data}(M) - F_2^{data}(M)$
- cumulative variable of transverse momentum
  - transforms non-uniform single-particle distribution into a uniform one ranging from 0 to 1
  - remove the dependence of F_r on the shape of the single-particle distribution
  - intermittency index of an ideal power-law correlation function system described in two dimensions in momentum space was proven to remain approximately invariant after the transformation

Released results of intermittency analysis

Pb+Pb at 13A GeV/c ($\sqrt{s_{NN}} \approx 5.1$ GeV)

Pb+Pb at 30A GeV/c ($\sqrt{s_{NN}} \approx 7.5$ GeV)

Ar+Sc at 13A-150A GeV/c ($\sqrt{s_{NN}} \approx 5.1$-17 GeV)

Cumulative variables
Independent sub-sample for each M points

Adhikary, H. (2022), arXiv. https://doi.org/10.48550/arXiv.2211.10504

Results of proton intermittency analysis

M range (1 . . . 150^2)

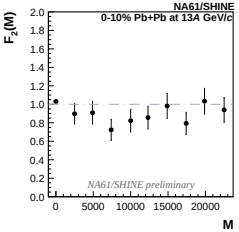

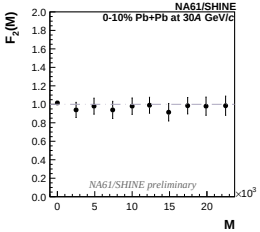

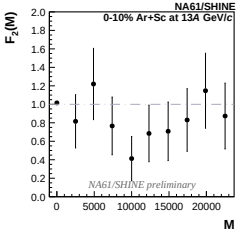

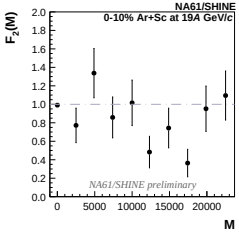

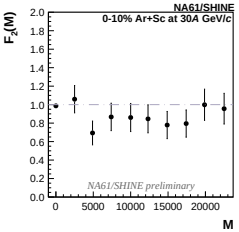

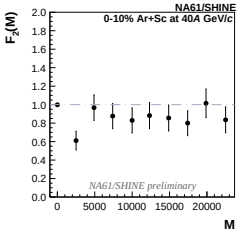

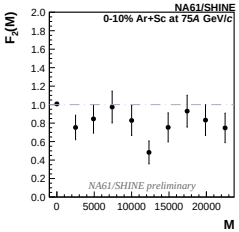

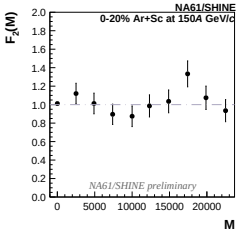

Adhikary, H. (2022), arXiv, https://doi.org/10.48550/arXiv.2211.10504

No indication for power-law increase with bin size and/or scaling

Results of proton intermittency analysis

limited M range (1 . . . 32^2)

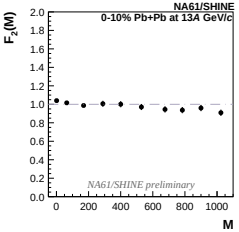

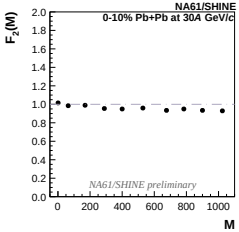

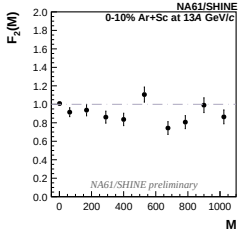

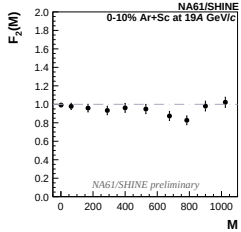

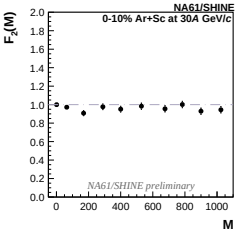

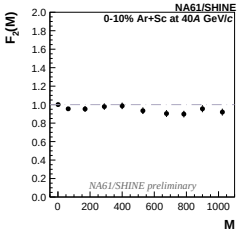

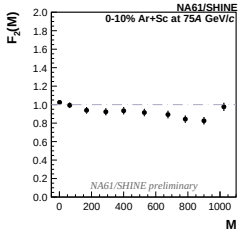

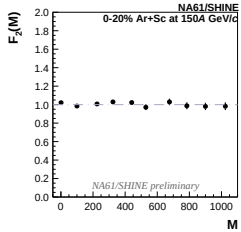

Adhikary, H. (2022), arXiv, https://doi.org/10.48550/arXiv.2211.10504

No indication for power-law increase with bin size and/or scaling

Ar+Sc energy scan results

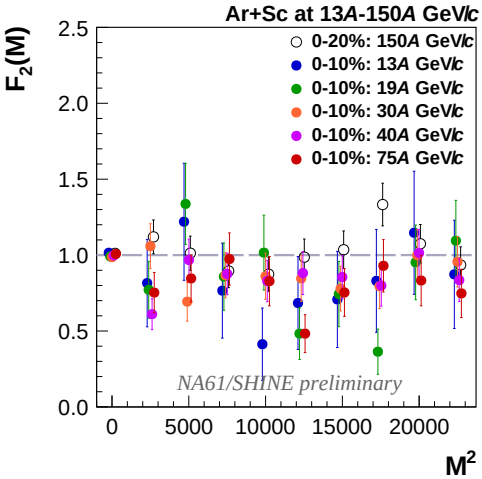

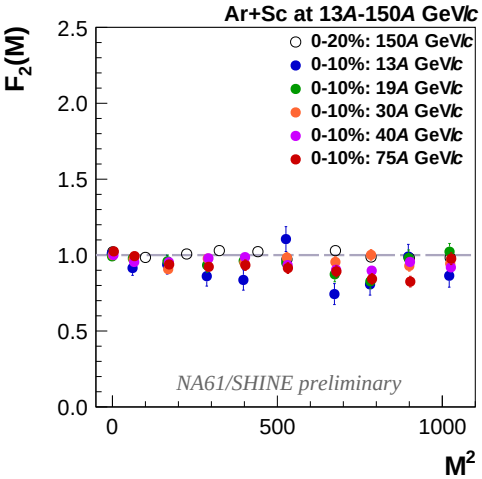

- - - No indication for power-law increase with bin size - - -

* M points are slightly shifted for different energies to increase readability *

Comparison with EPOS

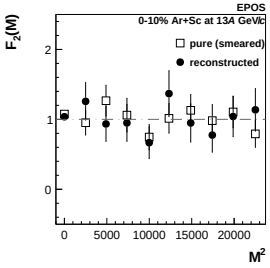

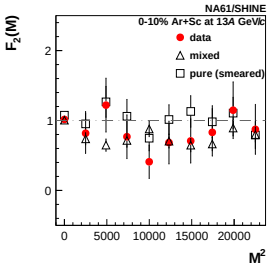

Goal: comparison of experimental data with EPOS model and estimate systematic bias:

0-10% central Ar+Sc data sets are generated with **EPOS 1.99**. Signals from the NA61/SHINE detector were simulated with GEANT3 software, and the recorded events were reconstructed using the standard NA61/SHINE procedure:

- **pure EPOS (for model predictions):** 60% accepted protons and protons pairs within the single and two-particle acceptance map from EPOS generated 0-10% central events
- **reconstructed EPOS:** selected protons and proton pairs were subject to the same cuts as used for the experimental data analysis from EPOS model events (have reconstructed primary vertex)
- **Momententum resolution:** Impact of momentum resolution may be significant in the case of critical correlation; thus, a comparison with EPOS requires smearing of momentum component according to the experimental resolution (pure smeared)

Summary:

- Biases of the experimental data are significantly smaller than the statistical data uncertainties
- Experimental results are compared with the pure EPOS, and no significant differences are observed for Ar+Sc at 13*A*-150*A* GeV/*c*

Simple power-law model

A simple model generates events, that reproduce the experimental multiplicity and transverse momentum distributions of particles

Correlated pairs (signal)

$$\rho(|\Delta\vec{p}_T|) = (|\Delta\vec{p}_T|)^{-\varphi}$$

It has two main parameters:

- ratio of correlated to uncorrelated particles
- power-law exponent

Lots of model data sets are generated:

- correlated-to-all ratio: vary from 0.0 to 4.0%(with 0.2% step)
- power-law-exponent: vary from 0.0 to 1.0 (with 0.05 step)

and compared with the experimental data

For the construction of exclusion plots, statistical uncertainties were calculated using model with statistics corresponding to the data.

M = 1 . . . 150^2

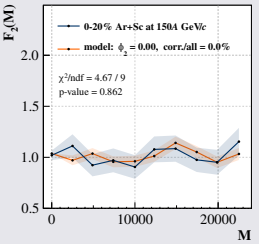

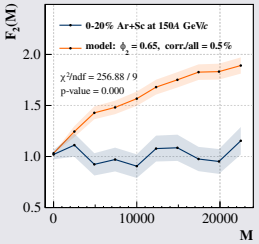

Exclusion plots from a simple power-law model

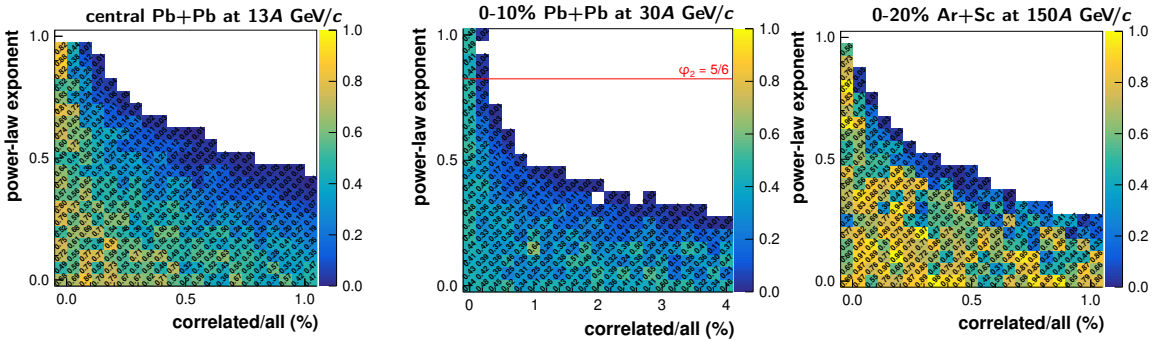

white area: p-value < 0.01

exclusion plots for parameters of simple power-law model

The intermittency index φ_2 for a system freezing out at the critical endpoint is expected to be φ_2=5/6 assuming that it belongs to the 3-D Ising universality class

Summary of NA61/SHINE critical point search

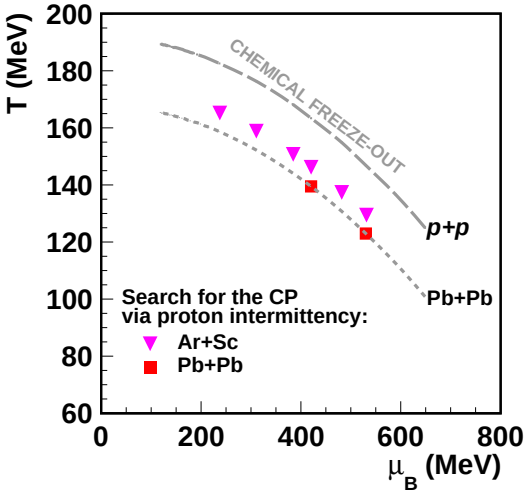

- Summarize NA61/SHINE critical point search via proton intermittency on the diagram of chemical freeze-out temperature and chemical potential
- Dashed line indicates parameters in p+p interactions
- Dotted line in central Pb+Pb collisions
- Color points mark reactions in the T-μ_B phase diagram for which search for the critical point was conducted
- Freeze-out points in the T-μ_B achieved by simple parabolic fit within the statistical hadronization model (SHM) supplemented with the hydrodynamical expansion of the matter

F. Becattini, J. Manninen and M. Gazdzicki, Phys.Rev. C73 (2006) 044905

STAR vs NA61/SHINE preliminary results on ΔFq(M)

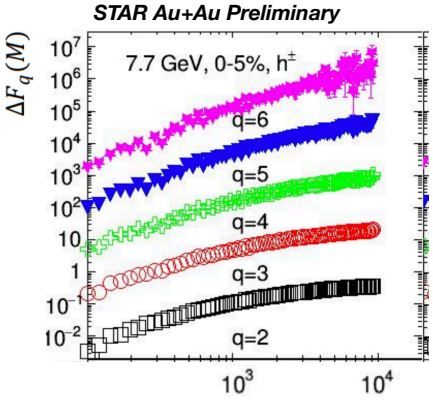

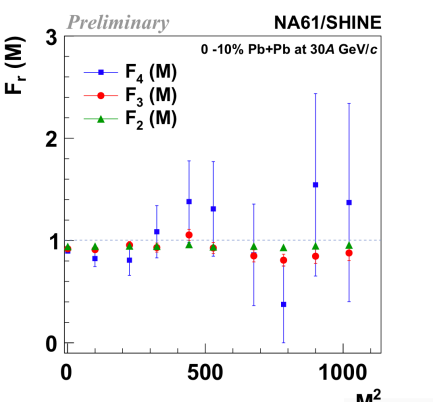

$$\Delta F_q(M) = F_q^{data}(M) - F_q^{mix}(M)$$

calculated for cumulative variables

h-

This seems to be in tension with corresponding results by the STAR Collaboration

NA61 vs STAR results

	STAR	NA61/SHINE
reaction	^{197}Au+^{197}Au	^{208}Pb+^{208}Pb
$\sqrt{s_{NN}}$ (GeV)	7.7, 11.5, 14.5, 19.6, 27, 39, 54.4, 62.4, 200	7.5
particles of interest	p, $\bar{p}$, $K^{\pm}$, $\pi^{\pm}$	all charged except $e^{\pm}$
efficiency	low, corrected for	not corrected
points	dependent	independent
background subtraction	mixed events	cumulative analysis
final result	$\nu(\sqrt{s_{NN}})$	$\Delta F_{2,3,4}(M)$

STAR results: arXiv:2301.11062v1 [nucl-ex] 26 Jan 2023

Tobiasz's compilation:
https://indico.cern.ch/event/1241273/contributions/5298704/attachments/2621677/4532908/TC_STARvsSHINE_2023-03-31.pdf

STAR analysis proceedure

$$F_q(M) = \frac{< \frac{1}{M^D} \sum_{i=1}^{M^D} n_i(n_i-1)\dots(n_i-q+1) >}{< \frac{1}{M^D} \sum_{i=1}^{M^D} n_i >^q}$$

$$\Delta F_q(M) = F_q^{data}(M) - F_q^{mix}(M) \sim (M^2)^{\phi_q}$$

More study:

$$\Delta F_q(M) \propto \Delta F_2(M)^{\beta_q}$$

$$\beta_q \propto (q-1)^{\nu}$$

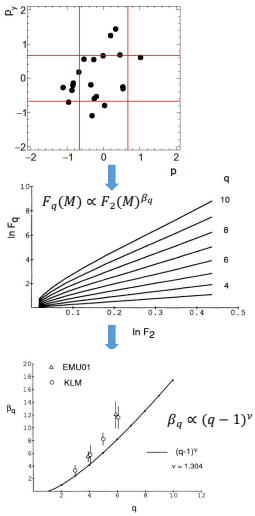

- $F_q(M)$ in transverse momentum space (p_x-p_y).
- Charged particles (p, $\bar{p}$, $\pi^{\pm}$, $K^{\pm}$) and protons (p, $\bar{p}$).
- Looking for $\boldsymbol{F_q(M)/M}$ **scaling and** $\boldsymbol{F_q(M)/F_2(M)}$ **scaling**.
- **Energy and centrality dependence of** $\boldsymbol{\nu}$ in Au + Au collisions at $\sqrt{s_{NN}}$ = 7.7 - 200 GeV.

Compare STAR result

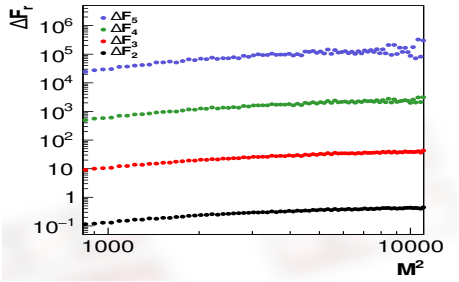

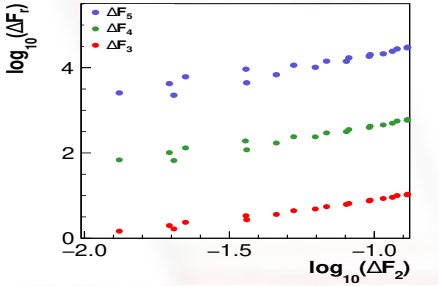

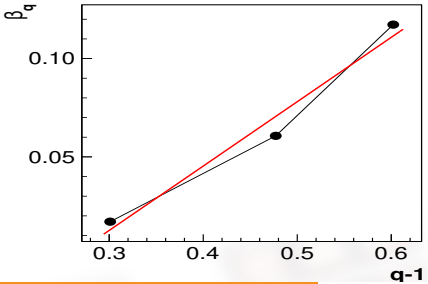

$\nu_{NA61/SHINE} \approx 0.33$

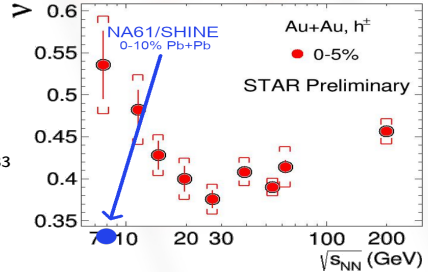

Summary

Results on **proton intermittency** analysis with second scaled factorial moments for **uncorrelated points** using **non-cumulative** and **cumulative variables** in inelastic Pb+Pb collisions at 13A, 30A GeV/c and Ar+Sc collisions at 13A - 75A GeV/c has been presented

- If the system freeze-out in the vicinity of the critical point, scaled factorial moments should exhibit a power-law dependence on bin number
- Using cumulative quantities removes dependence on the shape of the single-particle distribution while preserving critical behavior
- Protons are selected with a simple graphical cut based on theoretical Bethe-Bloch curves and accepted average 60% protons are selected with less than 4 % kaon contamination
- **No effect is observed by dE/dx cut of proton candidates selection test**
- The available phase-space region is described with a 3D map (y_p^{cms},p_x,p_y)
- Momentum based two track distance cut is applied
- **Biases of the experimental data are significantly smaller than the statistical data uncertainties**
- **Experimental results are compared with the pure EPOS, and no significant differences are observed for Pb+Pb at 13A, 30A GeV/c and Ar+Sc at 13A-75A GeV/c**
- **No indication for power-law increase with bin size is observed in Ar+Sc at 13A -150A GeV/c data by proton intermittency analysis**
- Exclusion plots for Ar+Sc at 13A-75A GeV/care preparing

Proton intermittency released result of Ar+Sc at 13A-75A GeV/c:
https://twiki.cern.ch/twiki/bin/view/NA61/Intermittency_cumulative_noncumulative

Proton intermittency preliminary released result of Pb+Pb at 30A GeV/c: https://twiki.cern.ch/twiki/bin/view/NA61/Intermittency_PbPb30A
Proton intermittency preliminary released result of Pb+Pb at 13A GeV/c: https://twiki.cern.ch/twiki/bin/view/NA61/Intermittency_PbPb13A

EUROPEAN ORGANISATION FOR NUCLEAR RESEARCH (CERN)

March 30, 2023

Search for the critical point of strongly-interacting matter in ^{40}Ar + ^{45}Sc collisions at 13A, 19A, 30A, 40A, and 75A GeV/c using scaled factorial moments of protons

Paper draft is ongoing...

The NA61/SHINE Collaboration

The critical point of dense, strongly interacting matter is searched for at the CERN SPS in ^{40}Ar + ^{45}Sc collisions at 13A, 19A, 30A, 40A, and 75A GeV/c. The dependence of second-order scaled factorial moments of proton multiplicity distribution on the number of subdivisions of transverse momentum space is measured. The intermittency analysis is performed using both transverse momentum and cumulative transverse momentum and statistically independent data sets are used for each subdivision number.

The obtained results do not indicate any statistically significant intermittency pattern. An upper limit on the fraction of critical proton pairs and the power of the correlation function is obtained based on a comparison with the Power-law Model [1] developed for this purpose.

PhD Thesis

PhD thesis is under review, expected to submit to PhD school by the end of June

Chapters:

1. Introduction
2. Intermittency analysis in high energy physic
3. Methodology of proton intermittency analysis
4. NA61/SHINE experiment
5. Analysis of NA61/SHINE data
6. Intermittency analysis results
7. Comparison with models
8. Summary

Thanks

Why intermittency analysis to search for the QCD critical point?

INTERMITTENCY AND CRITICAL BEHAVIOUR

Helmut SATZ

Theory Division, CERN, CH-1211 Geneva 23, Switzerland
and
Fakultät für Physik, Universität Bielefeld, D-48 Bielefeld, FRG

Received 9 March 1989

Following a brief introduction to intermittent behaviour, we show that the Ising model leads to intermittency at the critical point. The intermittency indices are given in terms of the critical exponents. This result is expected to hold for second-order phase transitions in general; for finite temperature SU(2) gauge theory, it follows from universality.

- J. Wosiek has found a hint for intermittent behaviour in the critical region of the two-dimensional Ising model
- This suggested the general question: what, if any, relation is there between intermittency and critical behaviour?
- The answer is of interest also for the study of high-energy nuclear collisions, in which one hopes to find evidence for the transition from HM to QGP

Why proton intermittency analysis to search for QCD critical point?

VOLUME 91, NUMBER 10 PHYSICAL REVIEW LETTERS week ending 5 SEPTEMBER 2003

Proton-Number Fluctuation as a Signal of the QCD Critical End Point

Y. Hatta
Department of Physics, Kyoto University, Kyoto 606-8502, Japan
and The Institute of Physical and Chemical Research (RIKEN), Wako, Saitama 351-0198, Japan

M. A. Stephanov
Department of Physics, University of Illinois, Chicago, Illinois 60607-7059, USA
and RIKEN-BNL Research Center, Brookhaven National Laboratory, Upton, New York 11973, USA
(Received 11 February 2003; published 4 September 2003; publisher error corrected 8 September 2003)

We argue that the event-by-event fluctuation of the proton number is a meaningful and promising observable for the purpose of detecting the QCD critical end point in heavy-ion collision experiments. The long range fluctuation of the order parameter induces a characteristic correlation between protons which can be measured. The proton fluctuation also manifests itself as anomalous enhancement of charge fluctuations near the end point, which might be already seen in existing data.

DOI: 10.1103/PhysRevLett.91.102003 PACS numbers: 12.38.–t, 11.10.Wx, 25.75.–q

- Protons carry both the baryon and electric charges. They are sensitive to the fluctuation of the order parameter
- At the critical end-point, the singularity of the baryon number susceptibility is completely reflected in the proton numbers fluctuation

Why intermittency analysis in transverse momentum space

PRL 97, 032002 (2006) PHYSICAL REVIEW LETTERS week ending 21 JULY 2006

Critical Opalescence in Baryonic QCD Matter

N. G. Antoniou, F. K. Diakonos,* and A. S. Kapoyannis
Department of Physics, University of Athens, 15771 Athens, Greece

K. S. Kousouris
National Research Center "Demokritos," Institute of Nuclear Physics, Aghia Paraskevi, 15310 Athens, Greece
(Received 19 January 2006; published 21 July 2006)

We show that critical opalescence, a clear signature of second-order phase transition in conventional matter, manifests itself as critical intermittency in QCD matter produced in experiments with nuclei. This behavior is revealed in transverse momentum spectra as a pattern of power laws in factorial moments, to all orders, associated with baryon production. This phenomenon together with a similar effect in the isoscalar sector of pions (sigma mode) provide us with a set of observables associated with the search for the QCD critical point in experiments with nuclei at high energies.

DOI: 10.1103/PhysRevLett.97.032002 PACS numbers: 12.38.Mh, 05.70.Jk

- Intermittency attempts to detect a geometrical fractal structure in the fireball created by the collision; evolution of the system in time degrades this structure, and the deformation is much more severe in the longitudinal direction than in the transverse one
- In case of intermittency analysis in rapidity distribution, in the longitudinal direction, there is a possibility of string branching, which can give a possible power-law signal

Why analysis in mid-rapidity region?

Search for critical fluctuations of the proton density in central A+A collisions at maximum SPS energy

Research Article

Nikolaos G. Antoniou[1] *, Nikos Davis[1] †, Fotis K. Diakonos[1] ‡ (for the NA49 Collaboration)

1 *University of Athens, Department of Physics, GR-15771 Athens, Greece*

Received Jan 23, 2012; accepted Sep 16, 2012

Abstract: We performed an intermittency analysis of the proton density fluctuations in transverse momentum space for the collisions Si+A (A=Al,Si,P) and C+A (A=C,N) at maximum SPS energy ($\sqrt{s_{NN}} \approx 17$ GeV). In our analysis we used exclusively proton tracks in the midrapidity region ($|y_{CM}| \leq 0.75$). For the Si+A system we find signature of power-law distributed density fluctuations quantified by the intermittency index ϕ_2 which approaches in size the predictions of critical QCD [Phys. Rev. Lett. 97, 032002 (2006)]. This result supports further the recent findings of power-law fluctuations in the density of (π^+, π^-) pairs with invariant mass close to their production threshold for the Si+Si at the same energy, reported in [Phys. Rev. C 81, 064907 (2010)].

The critical intermittency index is determined from the first principle (universality class arguments) and it is valid for protons produced in the mid-rapidity region which is necessary for avoiding spectators in the considered data sets

Space-time picture of ultra-relativistic heavy-ion collisions

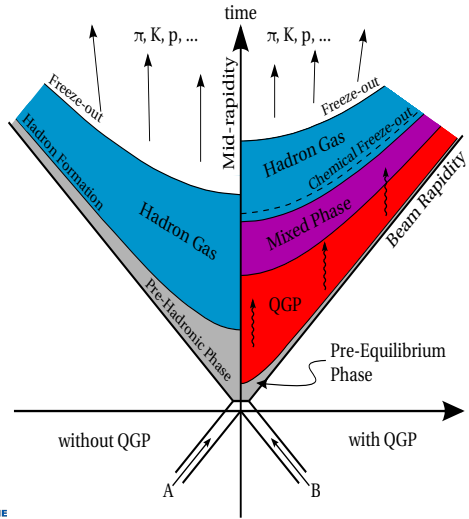

During the collision, the energy of the system increases and new particles can be produced in two ways:

- **Scenario-1:** energy density after the collision is relatively low, a hot and dense hadron gas is formed
- **Scenario-2:** energy density is sufficiently high, QGP can be created
  - **Hadronisation:** as QGP expands and cools down, the hadron formation process takes place
  - **Chemical freeze-out:** moment when the inelastic interactions stop and the chemical composition of the system becomes fixed
- **Thermal(kinetic) freeze-out:** particles of hadron gas produced in both scenarios still interact with each other elastically, while the system continues to cool down until the momenta of all particles are fixed and a thermal (kinetic) freeze-out occurs
- These hadrons and/or the products of their decays can be observed in high-energy experiments